

Photo-responsive self-assembly based on a water-soluble pillar[6]arene and an azobenzene-containing amphiphile in water

Danyu Xia, Guocan Yu, Jinying Li and Feihe Huang^{*}

*State Key Laboratory of Chemical Engineering, Department of Chemistry,
Zhejiang University, Hangzhou 310027, P. R. China
Fax and Tel: +86-571-8795-3189; Email address: fhuang@zju.edu.cn.*

Electronic Supplementary Information (17 pages)

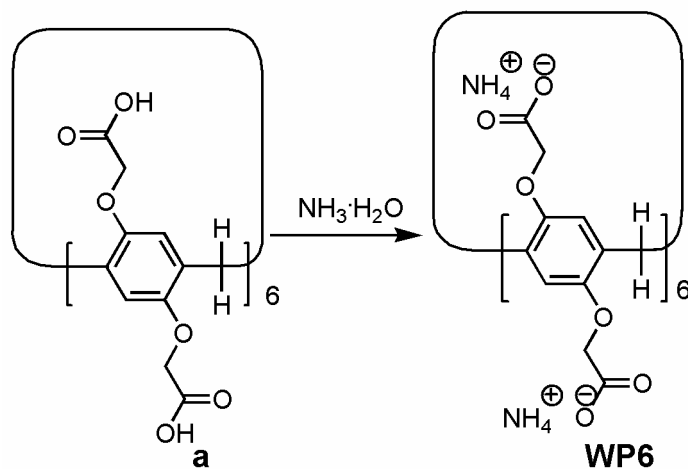
1. Materials and Methods	S2
2. Syntheses of water-soluble pillar[6]arene WP6 and guest 2	S3
3 Partial 2 D NOESY spectra of an equimolar solution of trans-1 and WP6	S7
4 Isothermal titration calorimetry (ITC) experiments	S8
5 UV-vis absorption spectroscopy experiments	S10
6 Critical aggregation concentration (CAC) determination of trans-2 and the equimolar mixture of trans-2 and WP6	S15
References	S17

1. Materials and methods

All reagents were commercially available and used as supplied without further purification. Compounds **1**^{S1}, **a**^{S2} and **b**^{S3} were prepared according to published procedures. NMR spectra were recorded with a Bruker Avance DMX 500 spectrophotometer or a Bruker Avance DMX 400 spectrophotometer. Low-resolution electrospray ionization mass spectra were recorded with a Bruker Esquire 3000 Plus spectrometer. High-resolution mass spectrometry experiments were performed with a Bruker 7-Tesla FT-ICR mass spectrometer equipped with an electrospray source (Billerica, MA, USA). The melting points were collected on a SHPSIC WRS-2 automatic melting point apparatus. UV-vis spectra were taken on a Perkin-Elmer Lambda 35 UV-vis spectrophotometer. Isothermal titration calorimetric (ITC) measurements were performed on a VP-ITC micro-calorimeter (Microcal, USA). The determination of the critical aggregation concentration (CAC) values was carried out on a DDS-307 instrument. Transmission electron microscopy investigations were carried out on a JEM-1200EX instrument. Dynamic light scattering was carried out on a Malvern Nanosizer S instrument at room temperature. Fluorescent microscopy investigations were carried out on an Axiovert 200 instrument.

2. Syntheses of water-soluble pillar[6]arene **WP6** and guest 2

2.1. Synthesis of water-soluble pillar[6]arene **WP6**



Scheme S1 Synthetic route to **WP6**

A solution of **a** (0.560 g, 0.390 mmol) and 40% $\text{NH}_3\cdot\text{H}_2\text{O}$ (40.0 mL) were stirred at reflux for 5 h. The mixture was concentrated under reduced pressure to get the precipitated product **WP6**. Then it was collected by filtration, washed with $\text{CH}_3\text{CH}_2\text{OH}$ and dried under vacuum to obtain **1** as a white solid (0.629 g, 99%). Mp: over 250 °C. The proton NMR spectrum of **WP6** is shown in Fig. S1. ^1H NMR (400 MHz, D_2O , room temperature) δ (ppm): 6.71 (s, 12H), 4.20 (s, 24H), 3.87 (s, 12H). The ^{13}C NMR spectrum of **WP6** is shown in Fig. S2. ^{13}C NMR (125 MHz, D_2O , room temperature) δ (ppm): 176.83, 150.11, 128.42, 115.89, 67.97, 30.08. LRESIMS is shown in Fig. S3: m/z 786.0 [$\text{M} - 2\text{NH}_3 - 4\text{NH}_4 + 2\text{Na}]^{2-}$ (100%). HRESIMS: m/z calcd for $[\text{M} - 2\text{NH}_4 - 10\text{NH}_3]^{2-}$ $\text{C}_{66}\text{H}_{58}\text{O}_{36}$, 713.1359, found 713.1351, error 1 ppm.

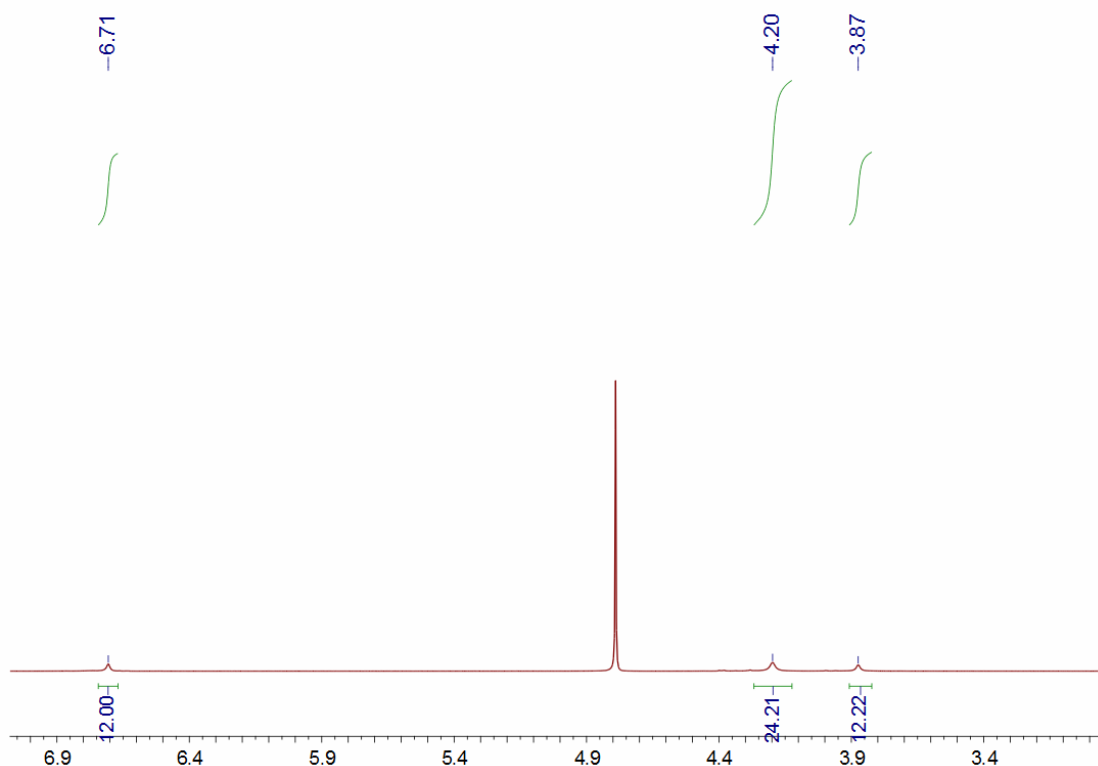


Fig. S1 ¹H NMR spectrum (400 MHz, D₂O, 298 K) of WP6.

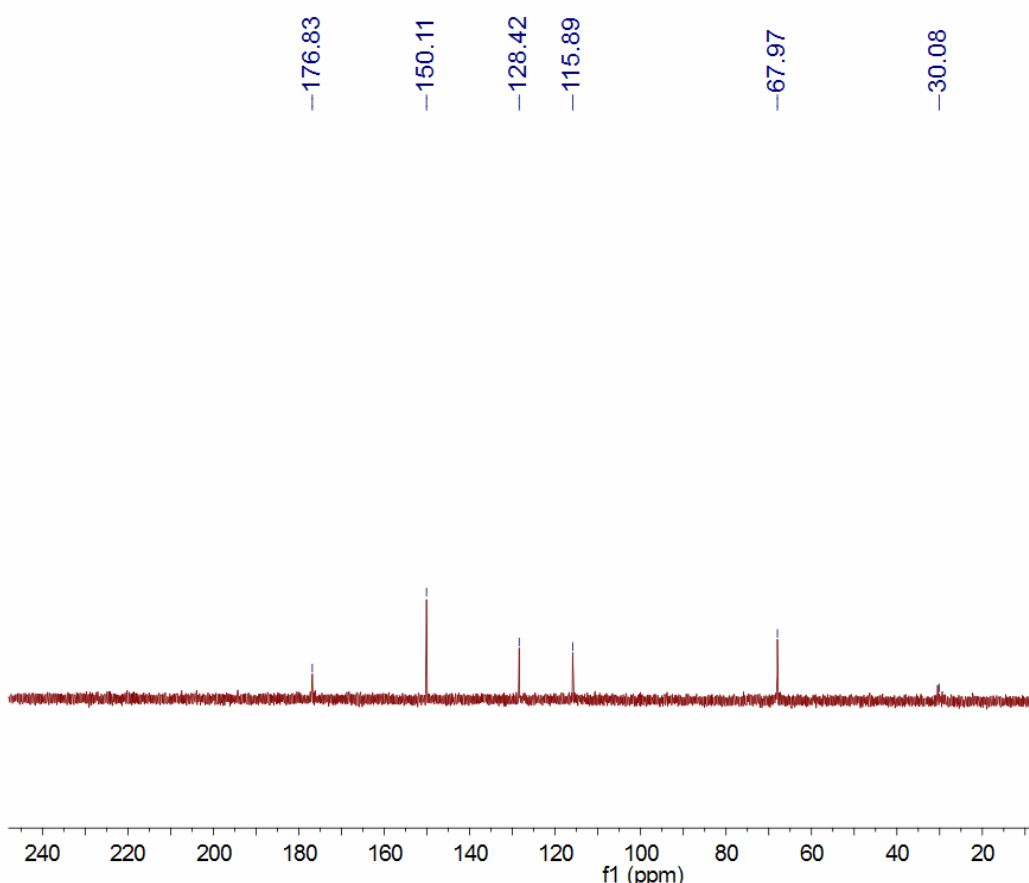


Fig. S2 ¹³C NMR spectrum (125 MHz, D₂O, 298 K) of WP6.

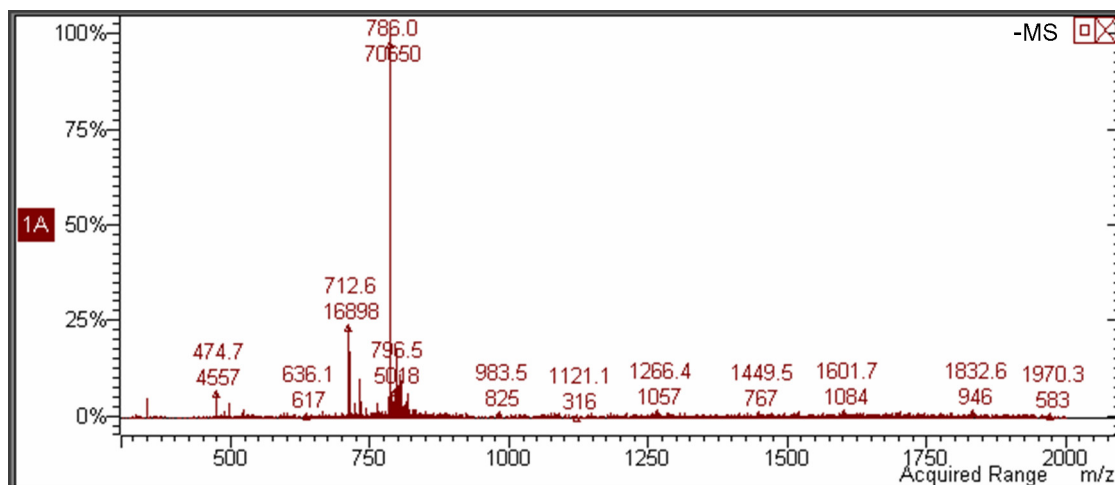
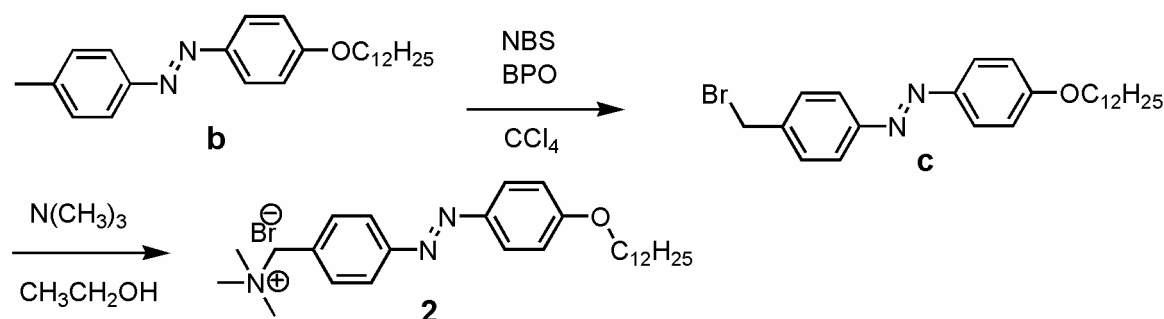


Fig. S3 Electrospray ionization mass spectrum of **WP6**. Main peak: m/z 786.0 [$M - 2\text{NH}_3 - 4\text{NH}_4 + 2\text{Na}^{2-}$] (100%).

2.2. Synthesis of guest **2**



Scheme S2 Synthetic route to **2**.

Synthesis of **c:** A mixture of **b** (1.25 g, 3.28 mmol), NBS (0.590 g, 3.28 mmol) and BPO (0.0300 g, 0.130 mmol) was stirred in CCl_4 at 77 °C under N_2 atmosphere for 24 h. The solution was evaporated under vacuum and the residue was purified by flash column chromatography on silica gel (petroleum ether) to obtain **2c** as an orange solid (1.31 g, 87%). A mixture of **c** (1.31 g, 2.85 mmol) and trimethylamine (33% in ethanol, 4.40 mL, 18.5 mmol) were added to ethanol (20.0 mL). The solution was refluxed overnight and was then evaporated under vacuum and the residue was purified by flash column chromatography on silica gel (petroleum ether/dichloromethane = 10/1, v/v) to obtain **c** as a yellow solid (1.40 g, 95%). mp: 206.5 – 208.0 °C. The ^1H NMR spectrum of compound **2** is shown in Fig. S3. ^1H NMR (400 MHz, CD_3CN , 298 K) δ (ppm): 7.94 (t, J = 8.6 Hz, 4 H), 7.66 (d, J = 8.4 Hz, 2 H), 7.08 (d, J = 8.8 Hz, 2 H), 4.46 (s, 2 H), 4.08 (t, J = 6.6 Hz, 2 H), 3.04 (s, 9 H), 1.27 (s, 20 H), 0.87 (t, J = 6.8 Hz, 3 H). The ^{13}C NMR spectrum of **2** is shown in Fig. S4. ^{13}C NMR (125

MHz, CD₃CN, 298 K) δ (ppm): 162.20, 153.55, 146.27, 133.65, 129.03, 124.67, 122.41, 114.70, 68.47, 68.12, 52.18, 52.15, 52.12, 29.03, 128.07, 123.22, 115.07, 114.24, 114.15, 113.96, 67.82, 55.84, 55.80, 55.77, 55.72. LRESIMS is shown in Fig. S5: *m/z* 437.9 [M – Br]⁺ (100%). HRESIMS: *m/z* calcd for [M – Br]⁺ C₂₈H₄₄N₃O, 438.3484, found 438.3474, error 2 ppm.

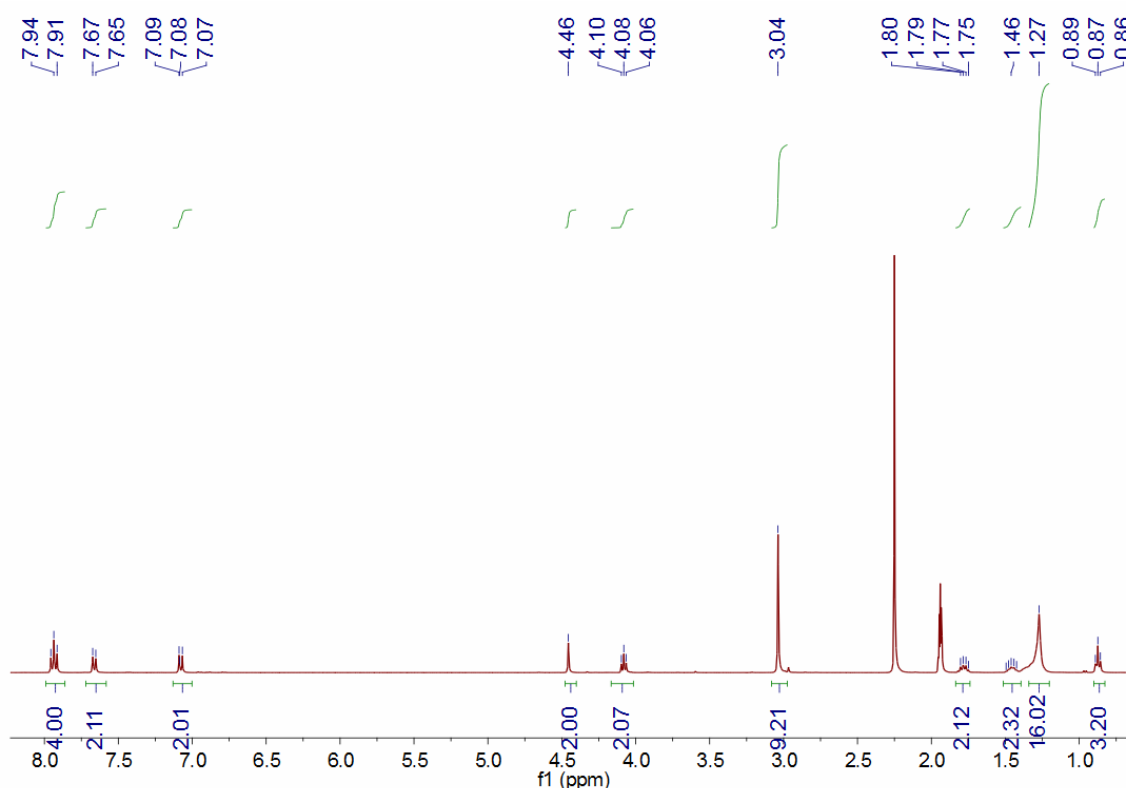


Fig. S4 ^1H NMR spectrum (400 MHz, CD_3CN , 298 K) of **2**.

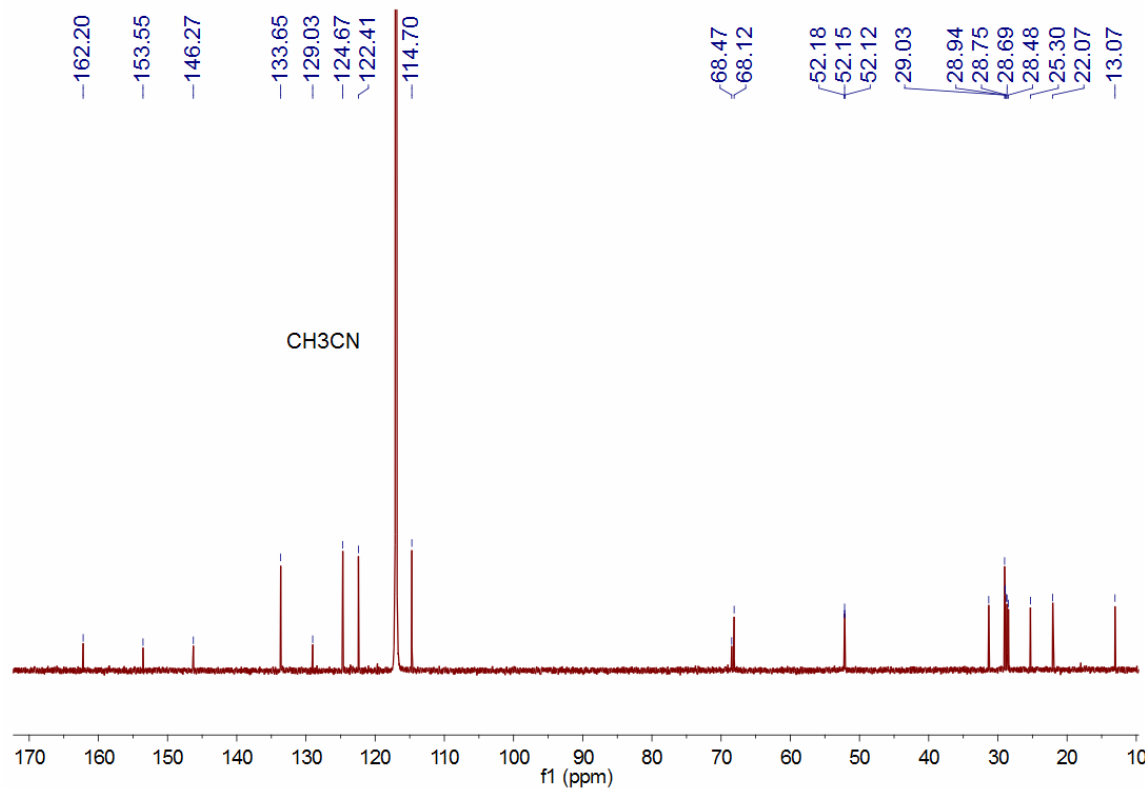


Fig. S5 ^{13}C NMR spectrum (125 MHz, CD₃CN, 298 K) of **2**.

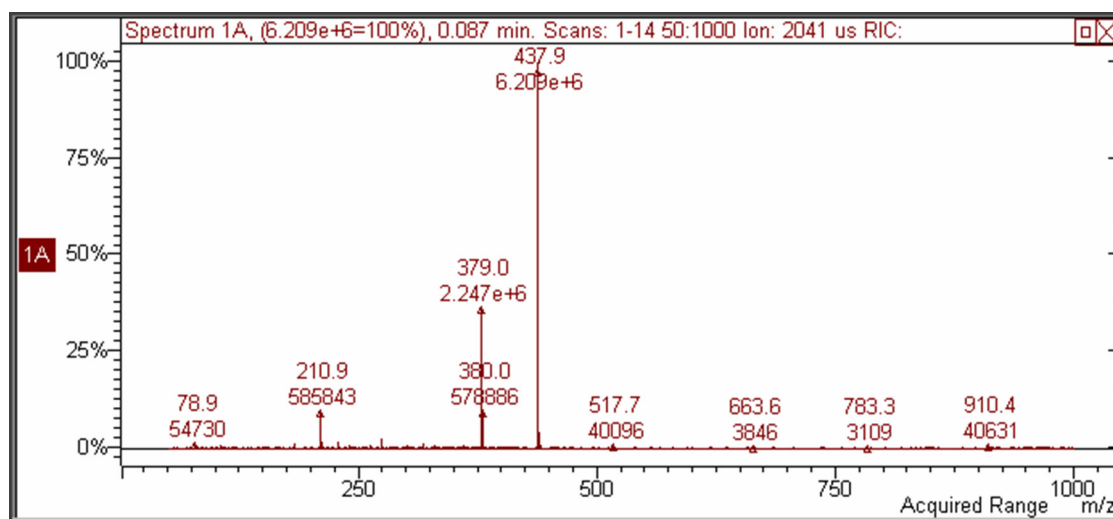


Fig. S6 Electrospray ionization mass spectrum of **2**. Main peak: m/z 437.9 [M – Br]⁺ (100%).

3. Partial 2 D NOESY spectra of an equimolar solution of *trans*-**1** and **WP6**

2 D NOESY NMR experiment was employed to study the relative positions of the components in complex **WP6**↔*trans*-**1**. NOE correlation signals were observed between protons H_e and H_c on the azobenzene unit of *trans*-**1** and proton H₁ of **WP6**

(Fig. S7, A and B) and between protons H_e, H_f, and H_g on the azobenzene unit of **trans-1** and proton H₂ of **WP6** (Fig. S7, C and D).

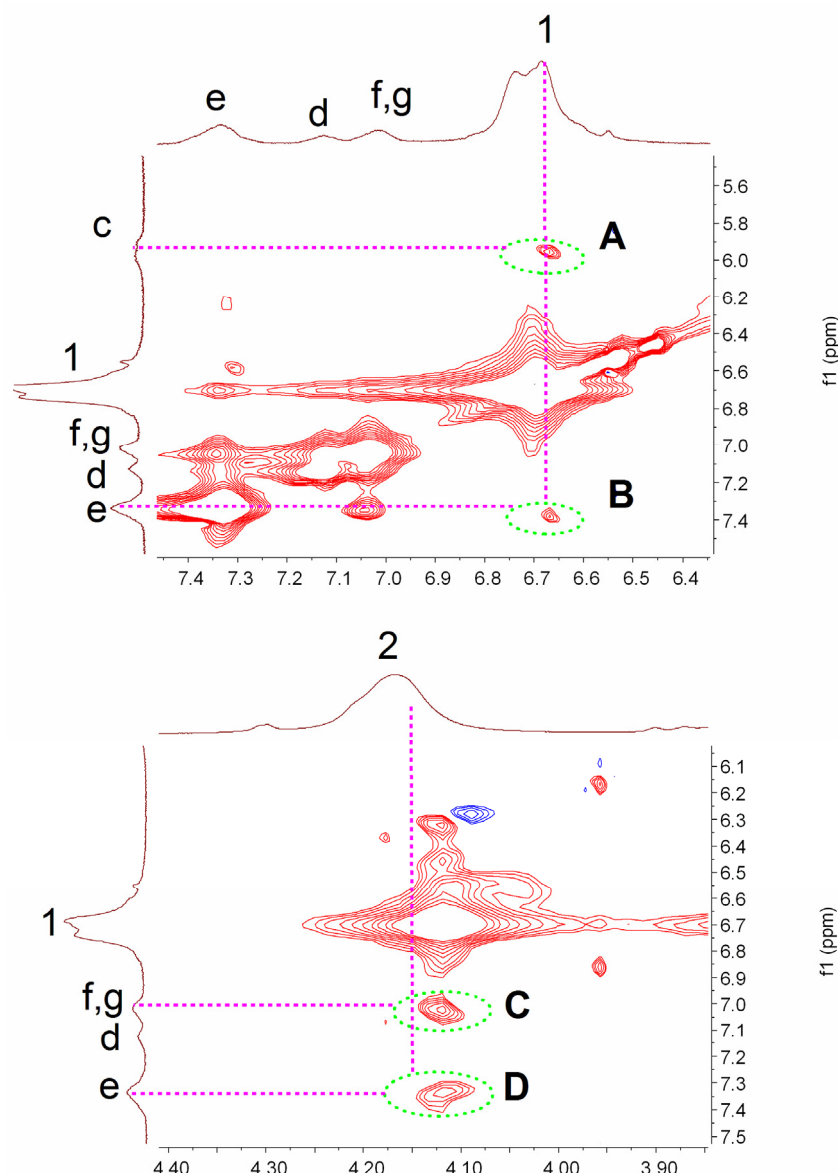


Fig. S7 Partial 2D NOESY spectra (500 MHz, D_2O , room temperature) of an equimolar mixture **trans-1** and **WP6** (2.50 mM).

4. Isothermal titration calorimetry (ITC) experiments

ITC is a useful tool to study the association constant (K_a), stoichiometry of host-guest complexes and thermodynamic parameters (enthalpy change ΔH° and entropy change ΔS°). As shown in Fig. S8, the enthalpy and entropy changes of **WP6**•**trans-1** were obtained ($\Delta H^\circ < 0$; $T\Delta S^\circ > 0$; $|\Delta H^\circ| > |T\Delta S^\circ|$), indicating that this complexation was driven by enthalpy changes with entropic assistance.

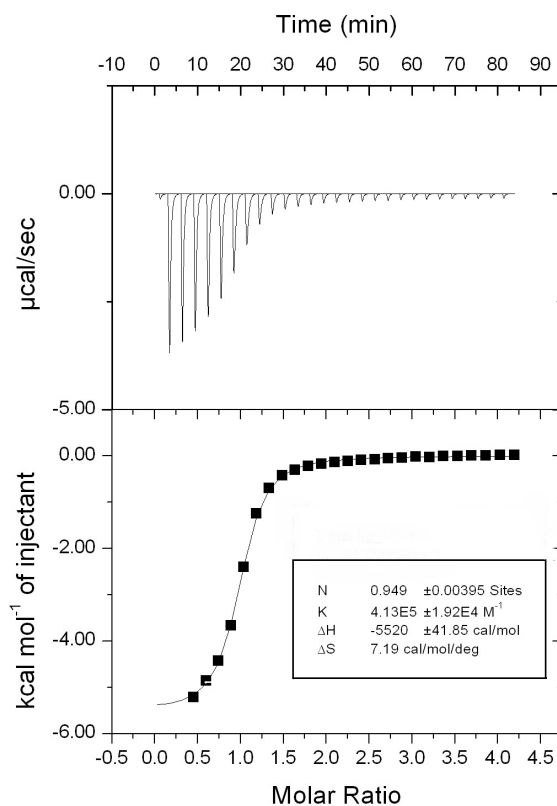


Fig. S8 Microcalorimetric titration of **WP6** with **trans-1** in water at 298.15 K. (Top) Raw ITC data for 29 sequential injections (10 μ L per injection) of a **trans-1** solution (2.00 mM) into a **WP6** solution (0.100 mM). (Bottom) Net reaction heat obtained from the integration of the calorimetric traces.

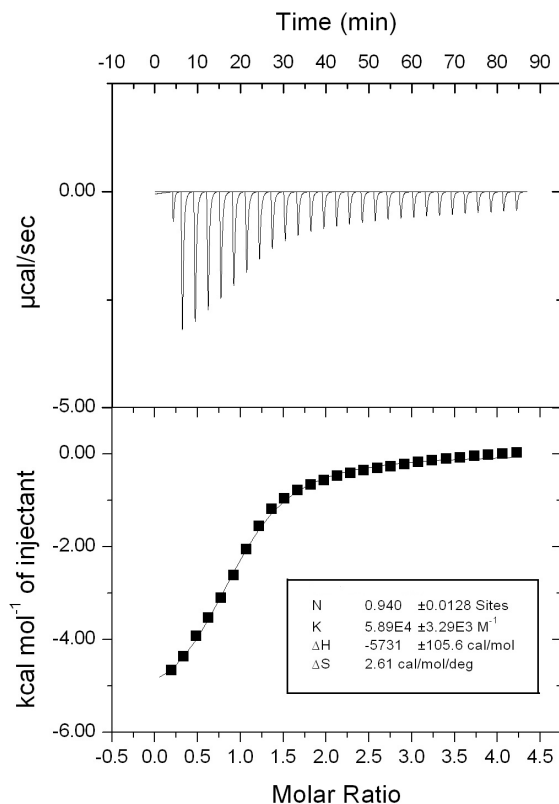


Fig. S9 Microcalorimetric titration of **WP6** with **trans-1/cis-1** (molar ratio 30/70) in water at 298.15 K. (Top) Raw ITC data for 29 sequential injections (10 μL per injection) of a **trans-1/cis-1** (molar ratio 30/70) solution (2.00 mM) into a **WP6** solution (0.100 mM). (Bottom) Net reaction heat obtained from the integration of the calorimetric traces.

5. UV-vis absorption spectroscopy experiments

UV-vis absorption spectroscopy was employed to study the photo-responsive properties of azobenzene-containing guest **2** (Fig. S10–S12). Upon irradiation with UV light at 365 nm, the absorption band at around 340 nm decreased dramatically, accompanied with the enhancement of the band around 435 nm indicating the photoisomerization from the *trans* state to the *cis* state. The absorption bands of the azobenzene unit at about 340 and 435 nm are ascribed to $\pi-\pi^*$ and $n-\pi^*$ transitions, respectively. Meanwhile, converse results were observed. As the photoisomerization of the azobenzene group proceeds with first-order kinetics in solution,^{S4} through plotting the changes of absorbance versus time, the initial *trans-cis* photoisomerization rate constant (k_t) was determined to be $(4.17 \pm 0.40) \times 10^{-2} \text{ s}^{-1}$, $(1.98 \pm 0.14) \times 10^{-2} \text{ s}^{-1}$ and $(0.966 \pm 0.075) \times 10^{-2} \text{ s}^{-1}$ in the absence and presence of 0.5 and 1.0 equiv of **WP6**, respectively (Fig. S13). The reason for the decrease of k_t values is that **trans-2** molecules freely dispersed in solution so that they can undergo

the *trans*-*cis* conversion easily. When **WP6** was added into the solution of **trans-2**, an inclusion complex **WP6**•**trans-2** formed, causing the complexed **trans-2** molecules geometrically restricted which will take time to disassociate from the host **WP6**.^{S4,S5} On the other hand, upon alternately irradiation with light at 365 and 435 nm of the solution of equimolar **WP6** and **trans-2**, the reversible photoisomerization process could be recycled many times (Fig. S10), suggesting that the threading-dethreading switch could be controlled reversibly.

5.1. Photo-responsive ability of 2

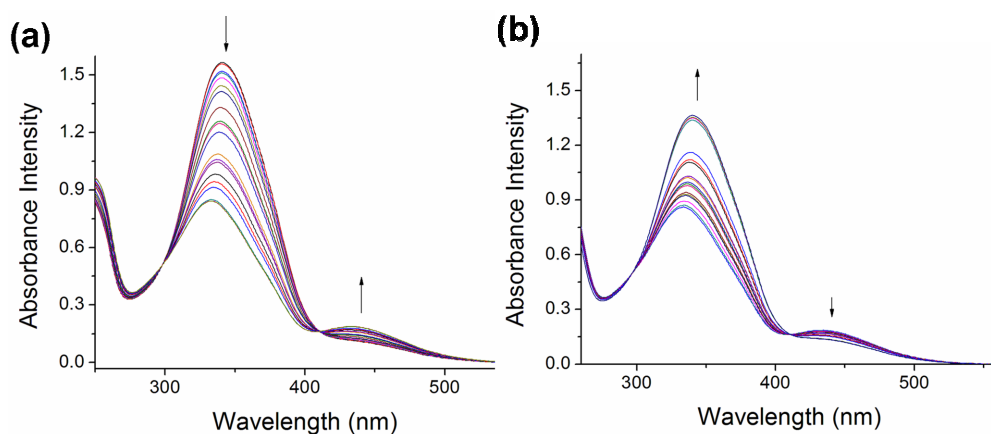


Fig. S10 UV-vis absorption spectra of **trans-2** in water under UV irradiation at 365 nm from 0 to 640 s (a) and upon visible irradiation at 435 nm from 0 to 640 s (b). The concentration of **trans-2** was 5.00×10^{-5} M.

5.2. The photo-controlled threading-dethreading switch between **2** and **WP6**

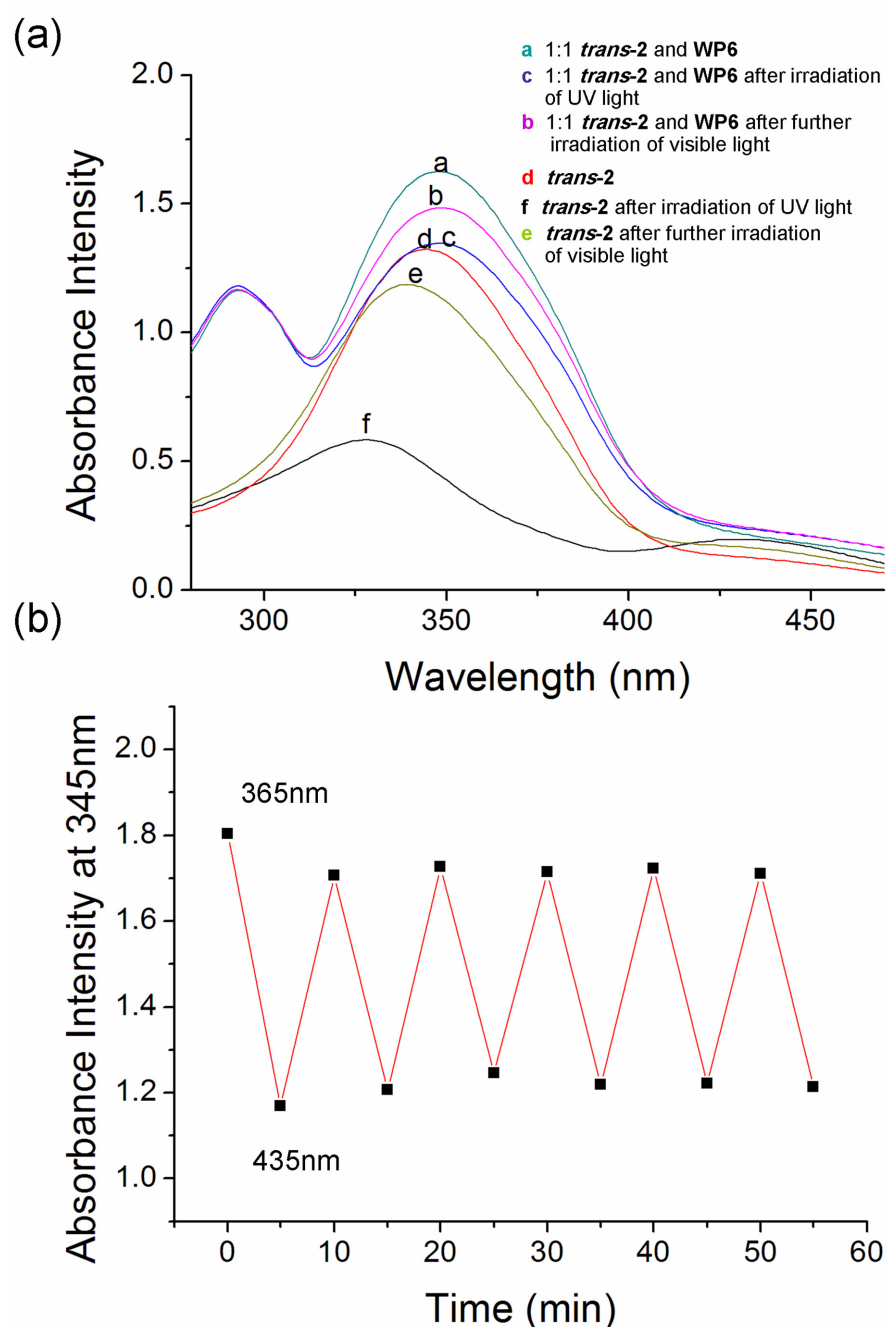


Fig. S11 (a) UV-vis spectra of 1.00×10^{-4} M *trans*-**2** (initial and after irradiation with UV light at 365 nm for 10 min) and solution of equimolar 1.00×10^{-4} M *trans*-**2** and **WP6** (initial, after irradiation with UV light at 365 nm for 10 min, and then after irradiation with visible light at 435 nm for 10 min) and (b) changes of the absorbance at 345 nm of an equimolar solution of **WP6** and *trans*-**2** upon alternating irradiation with UV and visible light for 10 min.

5.3. The photoisomeric behaviors of *trans*-**2** and the mixtures of **WP6** and **2**

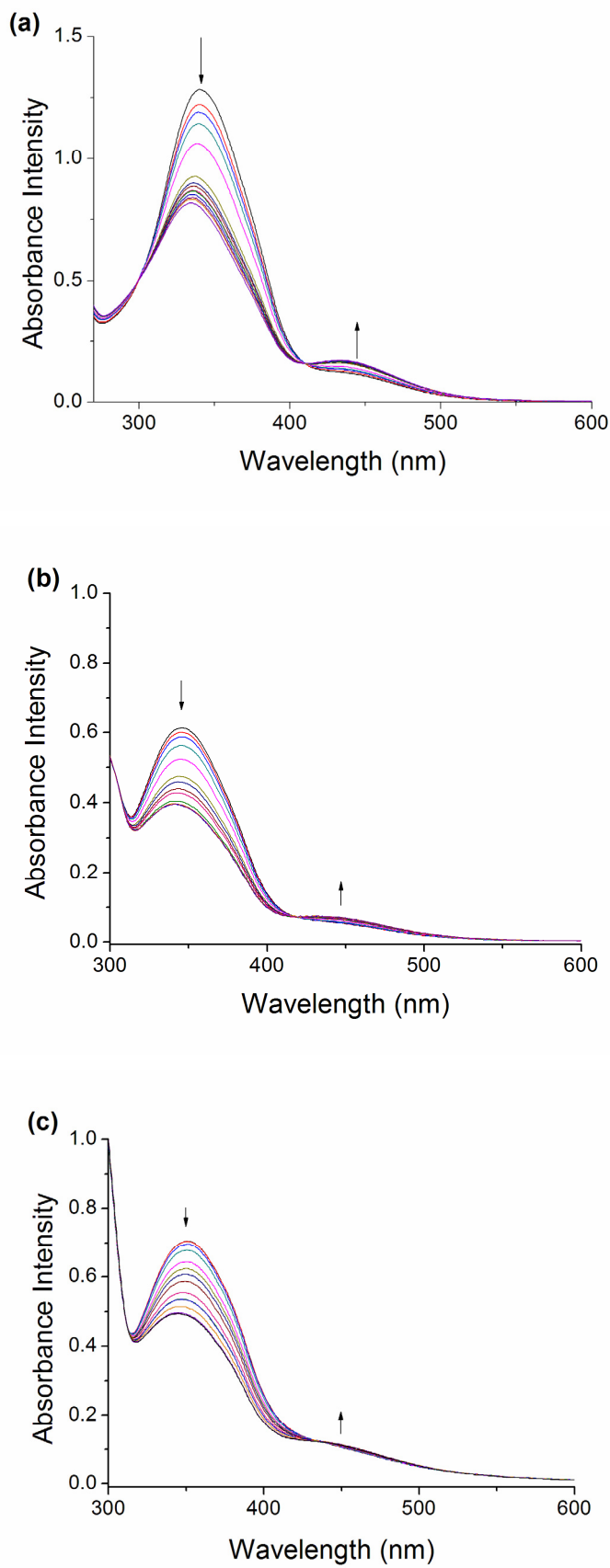


Fig. S12 UV-vis absorption spectra: (a) ***trans*-2**, (b) a mixture of ***trans*-2** and **WP6** (molar

ratio, 1:0.5); (c) a mixture of **trans-2** and **WP6** (molar ratio, 1:1). These water solutions were irradiated with UV light at 365 nm from 0 to 640 s. The concentration of **trans-2** was 5.00×10^{-5} M.

The first-order plots for the *trans*-*cis* photoisomerization of **trans-2** and mixtures of **WP6** and **trans-2** with different molar ratios are shown in Fig. S13 by the following equation: $y = y_0 + A \exp(-R_0 t)$.

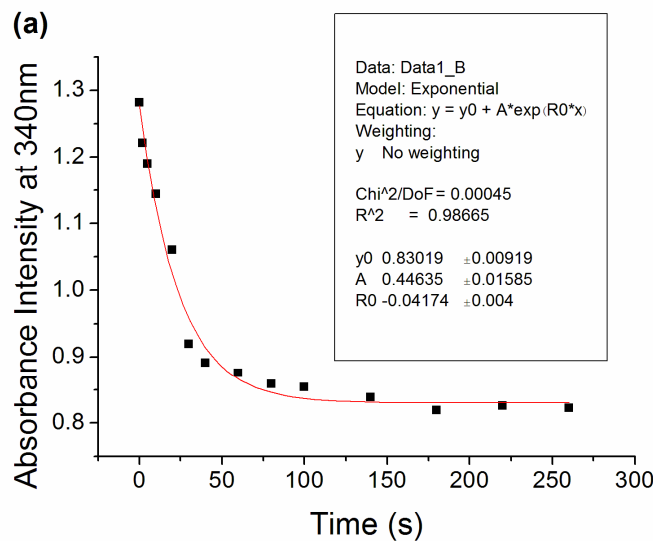
$$\ln \frac{A_0 - A_{eq}}{A_t - A_{eq}} = k_t t$$

$$\ln \frac{A_t - A_{eq}}{A_0 - A_{eq}} = -k_t t$$

$$\frac{A_t}{A_0 - A_{eq}} - \frac{A_{eq}}{A_0 - A_{eq}} = \exp(-k_t t)$$

$$A_t = A_{eq} + (A_0 - A_{eq})[\exp(-k_t t)]$$

It can be seen that where y is the absorbance A_t , x is the irradiation time t . y_0 is the absorbance at the photostationary state of azobenzene group at 365 nm, A is the absorbance intensity changes of the azobenzene group at 365 nm between the initial absorbance and the absorbance at the photostationary state. Therefore, y_0 and A are constant values, while $-R_0$ is the rate constant (k_t) of the *trans*-*cis* isomerization.



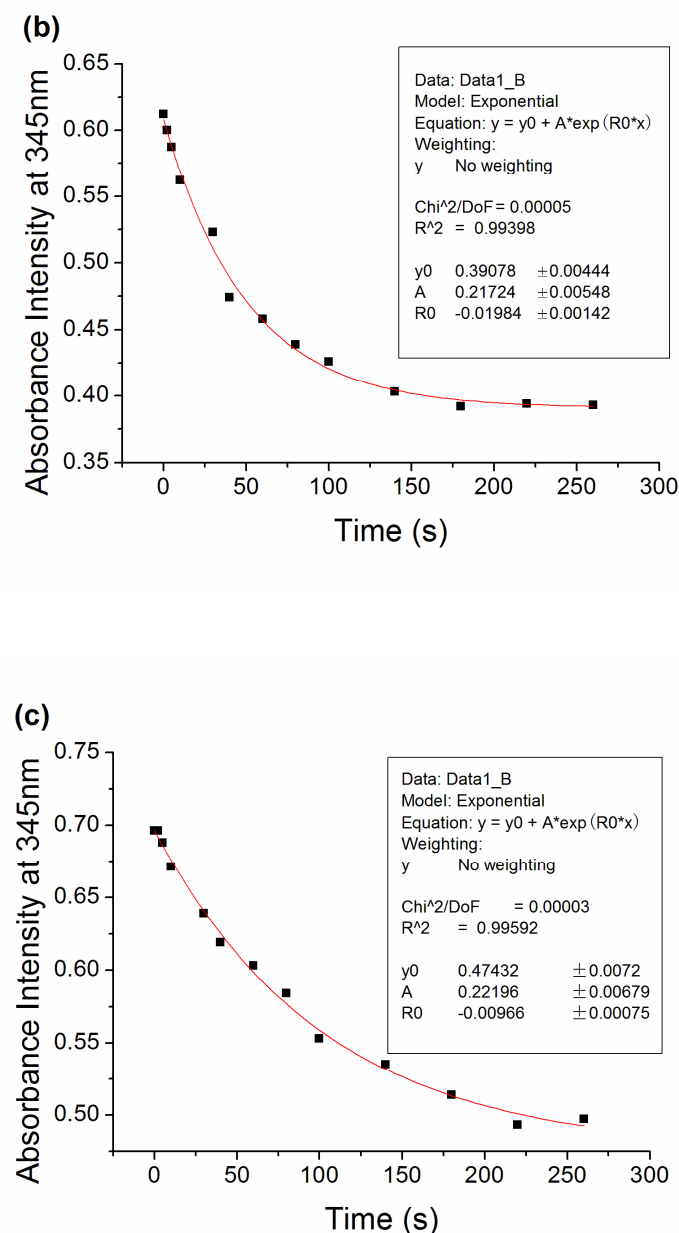


Fig. S13 Determination of the photoisomerization rate constants (k_t) upon being exposed to UV light at 365 nm in water: (a) for **trans-2**; (b) for **trans-2** and **WP6** (molar ratio, 1:0.5); (c) for **trans-2** and **WP6** (molar ratio, 1:1).

6. Critical aggregation concentration (CAC) determination of **trans-2** and the equimolar mixture of **trans-2** and **WP6**

To measure the CAC values of **trans-2** and the equimolar mixture of **trans-2** and **WP6**, the conductivities of the solutions at different concentrations of **trans-2** and the equimolar mixture of **trans-2** and **WP6** were determined. By plotting the conductivity versus the concentration, we estimated the CAC values of **trans-2** and the equimolar mixture of **trans-2**

and **WP6**.

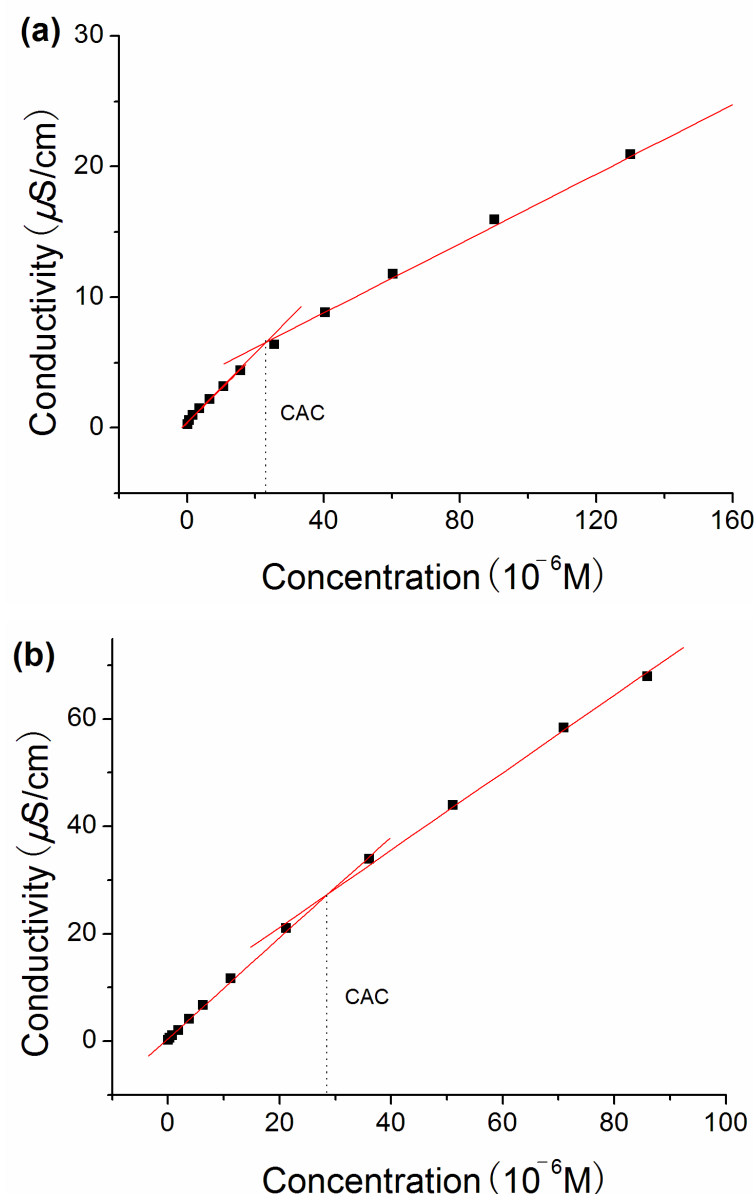


Fig. S14 (a) The concentration-dependent conductivity of **trans-2**. The critical aggregation concentration (CAC) was determined to be 2.19×10^{-5} M. (b) The concentration-dependent conductivity of the equimolar mixture of **trans-2** and **WP6**. The critical aggregation concentration (CAC) was determined to be 2.85×10^{-5} M.

References:

- S1. G. Yu, C. Han, Z. Zhang, J. Chen, X. Yan, B. Zheng, S. Liu and F. Huang, *J. Am. Chem. Soc.*, 2012, **134**, 8711–8717.
- S2. G. Yu, M. Xue, Z. Zhang, J. Li, C. Han and F. Huang, *J. Am. Chem. Soc.*, 2012, **134**, 13248–13251.
- S3. R. Bartolino, G. Coddens, F. Rustichelli, M. C. Pagnotta, C. Versace, M. Ghedini and F. Neve, *Molecular Crystals and Liquid Crystals*, 1992, **221**, 101–108.
- S4. Y. Wang, N. Ma, Z. Wang and X. Zhang, *Angew. Chem. Int. Ed.*, 2007, **46**, 2823–2826.
- S5. T.-T.-T. Nguyen, D. Türp, D. Wang, B. Nölscher, F. Laquai and K. Müllen, *J. Am. Chem. Soc.*, 2011, **133**, 11194–11204.